Journal of Biomedical Optics

SPIEDigitalLibrary.org/jbo

Noninvasive high resolving power entangled photon quantum microscope

Sanjit Karmakar
Ronald E. Meyers
Yanhua Shih

SPIE

Noninvasive high resolving power entangled photon quantum microscope

Sanjit Karmakar,[a] Ronald E. Meyers,[b,*] and Yanhua Shih[a]
[a]University of Maryland, Baltimore County, Department of Physics, Baltimore, Maryland 21250, United States
[b]U.S. Army Research Laboratory, Adelphi, Maryland 20783, United States

Abstract. A noninvasive high resolving power quantum microscope would facilitate progress in the areas of research and development in biosciences as well as in the area of biomedical technology. Longer-wavelength microscopes, i.e., visible or near-infrared, can provide noninvasive features. On the other hand, shorter wavelengths, i.e., in the ultraviolet, can provide better resolving power. We propose the development of both a noninvasive and high resolving power quantum microscope by using two-color entangled photon ghost imaging technology. [DOI: 10.1117/1.JBO.20.1.016008]

Keywords: entangled photons; two-color; noninvasive; quantum microscope; ghost imaging.

Paper 140636PR received Sep. 30, 2014; accepted for publication Dec. 2, 2014; published online Jan. 8, 2015.

1 Introduction

Many key areas of research and development in the biosciences and biomedical technology areas are progressing rapidly. One of the more exciting areas is biomedical imaging. Unfortunately, the light from high-resolving microscopes tends to damage cells. A high resolving power noninvasive microscope, capable of imaging without damaging cells or tissues, would enable physicians and scientists to better see and understand tissue and organ function.

The resolving power of a microscope can be improved in several ways. One example was the development of confocal microscopes, which provided better resolving power as well as higher contrast with respect to standard wide-field microscopy. Two other approaches have been proposed and analyzed by Simon and Sergienko[1,2] to improve the resolution of standard confocal microscopy. In one of these approaches, Simon and Sergienko used photon correlation, which improved resolution up to 50%.[1] In the other approach, they used a degenerate entangled photon pair generated from spontaneous parametric down-conversion (SPDC) to improve the resolution up to 77%.[2] Simon and Sergienko suggested the use of a nonlinear crystal after the object to illuminate the specimen with a high pump power to generate sufficient signal and idler photons. To obtain visible-light images with UV-level resolution, they also suggested the use of a UV pump to generate signal and idler photons in the visible range. However, because the specimen was illuminated by high-power UV light, there was a high probability of damaging the specimen, i.e., the cells and tissues studied in biomedical and biosciences.

In 1995 at UMBC, while investigating Einstein-Podolsky-Rosen phenomena, Pittman et al.[3] discovered ghost imaging using entangled photons to transmissively image a stencil mask internal to their experimental setup. Meyers et al.,[4,5] in 2007 and 2008, generated the first ghost image of a remote object by imaging a small toy soldier placed remotely from their setup at the Army Research Laboratory. This demonstration was the first practical application of ghost imaging, and it showed that ghost imaging could be applied to remote sensing from astrophysical to microscopic scales with the potential of increased resolution, increased contrast, and mitigation of adverse effects from distorting media. In 2010, Karmakar and Shih[6,7] reported on an experimental demonstration of two-color ghost imaging with enhanced resolving power. The resolution of two-color ghost imaging was also studied theoretically by Rubin and Shih[8] and Chan et al.[9] Certainly, disturbances around the object can degrade the image contrast of a microscope. However, in 2011, Meyers et al.[10,11] showed that disturbances, such as turbulence and distortions, do not affect multiphoton interference ghost imaging. While these studies used the quantum properties of thermal light, the Meyers et al. turbulence-free ghost imaging design also applies to entangled photons. In addition, absorption of photons by an object, though this leads to image information in conventional imaging, can potentially degrade the correlations in certain correlation-based imaging. An advantage of entangled photon imaging is that it eliminates most noise photons that can degrade correlation techniques and relatively few entangled photons are needed to accurately determine features.[3] However, accidental coincidences will form a noise background. With good detection equipment, accidental coincidences will be minimized. Furthermore, positive-negative ghost imaging techniques have been developed and experimentally verified, which achieve near 100% contrast by eliminating the effect of the noise background,[11,12] which improves images even using thermal light two-photon interference ghost imaging.

In this report, we propose a quantum microscope configuration capable of achieving high resolving power without any destruction of cells or tissues by using two-color ghost imaging technology. Such a quantum microscope configuration could provide improved image contrast and would not be affected by disturbances around the object.

2 Proposed Configuration

In the proposed experimental configuration, two-color ghost imaging technology is applied to improve the resolving power of a microscope system. Figure 1 shows a schematic

*Address all correspondence to: Ronald E. Meyers, E-mail: ronald.e.meyers6.civ@mail.mil

0091-3286/2015/$25.00 © 2015 SPIE

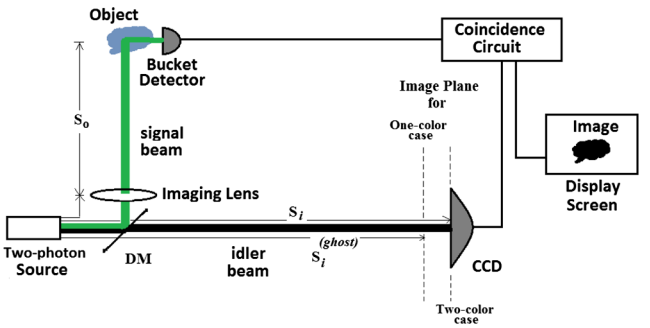

Fig. 1 Schematic of the experimental setup. DM is a dichroic mirror, which is used to separate two different colors of signal and idler beams.

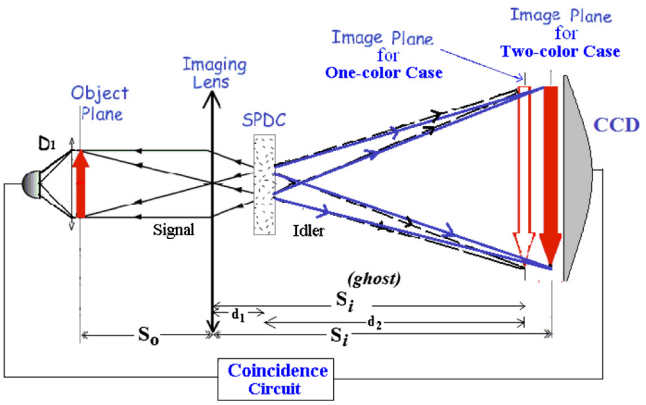

Fig. 2 Unfolded version of the experimental setup is shown to better understand the physics.[6,13]

of the experimental setup. By recording the joint-detection counts between the bucket detector and the CCD as a function of the transverse plane coordinates of the CCD in the idler beam, the image of the object aperture is observed with a magnification factor that is the same as the degenerate one-color case[3] as well as the classical case. In this experimental configuration, entangled photon pairs with $\lambda_s > \lambda_i$ generated from SPDC can reproduce a ghost image with enhanced resolving power by a factor of λ_s/λ_i by means of higher imaging amplification, where λ_s is the wavelength of the radiation that illuminates the object and λ_i is the wavelength of the idler beam. In this case, image amplification is enhanced by a factor of λ_s/λ_i more than that of the one-color ghost imaging or that of a classical imaging setup. Since the lowest limit of transparency of the nonlinear crystals for SPDC is ~190 nm, we propose the use of a 197-nm excimer laser as a pump. A type I BBO crystal together with this pump can be used as an entangled two-photon source to generate a signal beam of 695 nm in the visible range and an idler beam of 275 nm in the UV range. This configuration would improve the magnification power of a quantum microscope by a factor of 2.5. If one could produce a two-photon source capable of generating $\lambda_s \simeq 500$ nm in the visible region and $\lambda_i \simeq 1$ nm in the x-ray region, then the magnification power could be improved by a factor of 500.

3 Discussion and Analysis

In the two-color case, the signal and the idler photon pair from the SPDC source are emitted at different angles and opposite directions. Furthermore, if one photon is emitted at a certain angle, the emission angle of its conjugate is determined by the certain angle of that photon with unit probability. This permits us to explain the experiment in terms of geometrical optics by unfolding the schematic in Fig. 1 into that shown in Fig. 2 by considering the SPDC source as a hinge. The geometrical rays in Fig. 2 represent the two-photon amplitudes, therefore, the image is formed in terms of coincidence counts when the object aperture, imaging lens, and CCD are located according to the modified Gaussian thin lens equation. The relationship among the object aperture's optical distance from the lens, s_o, the image plane's optical distance from the lens, s_i (which is actually the distance from the lens back to SPDC source and then straight forward to the image plane), and the focal length of the imaging lens, f, satisfies a modified Gaussian thin-lens equation for two colors:[6,8]

$$\frac{\omega_s}{s_o}+\frac{\omega_i}{s_i}=\frac{\omega_s}{f} \quad \text{or} \quad \frac{1}{s_o}+\frac{1}{\frac{s_i}{d_1+d_2}\frac{\omega_s}{\omega_i}s_i^{(\text{ghost})}}=\frac{1}{f}, \tag{1}$$

where

$$s_i = d_1\frac{\omega_i}{\omega_s}+d_2 \quad \text{and} \quad s_i^{(\text{ghost})}=d_1+d_2, \tag{2}$$

and ω_s and ω_i are the angular frequencies of the signal and idler beam, respectively, and the Gaussian thin-lens equation in classical as well as in the degenerate case is

$$\frac{1}{s_o^O}+\frac{1}{s_i^O}=\frac{1}{f}, \tag{3}$$

where s_o^O and s_i^O are the object distance and image distance of the standard degenerate ghost imaging and classical imaging experimental setup.

By using the Glauber theory of photodetection, the joint detection probability between two detectors D_1 and CCD located at $(\mathbf{r}_1, t_1)$ and $(\mathbf{r}_2, t_2)$, respectively, can be expressed as follows:[14,15]

$$\begin{aligned} G^{(2)}(\mathbf{r}_1,t_1;\mathbf{r}_2,t_2) &= |\langle 0|\hat{E}_1^{(-)}\hat{E}_2^{(-)}\hat{E}_2^{(+)}\hat{E}_1^{(+)}|\Psi\rangle|^2 \\ &= |\Psi(\vec{\rho}_1,z_1,t_1;\vec{\rho}_2,z_2,t_2)|^2, \end{aligned} \tag{4}$$

where $\hat{E}_1^{(-)}$, $\hat{E}_2^{(+)}$ are the negative and positive frequency fields at space-time points $(\mathbf{r}_1, t_1)$ and $(\mathbf{r}_2, t_2)$, respectively, and $\Psi(\vec{\rho}_1, z_1, t_1; \vec{\rho}_2, z_2, t_2)$ is the two-photon amplitude, also called the two-photon effective wavefunction. Since imaging takes place on the transverse plane, we can calculate the transverse part of the two-photon effective wavefunction at the point $(z_1 = z_o, \vec{\rho}_1 = \vec{\rho}_o; z_2, \vec{\rho}_2)$:

$$\begin{aligned} \Psi(\vec{\rho}_o;\vec{\rho}_2) = \Psi_o \int d\vec{\kappa}_s d\vec{\kappa}_i \delta(\vec{\kappa}_s+\vec{\kappa}_i) \int d\omega_s\, d\omega_i \delta(\omega_s+\omega_i-\omega_p) \\ \times g(\vec{\kappa}_s,\omega_s;\vec{\rho}_o,z_o) g(\vec{\kappa}_i,\omega_i;\vec{\rho}_2,z_2), \end{aligned} \tag{5}$$

where $g(\vec{\kappa}_s, \omega_s; \vec{\rho}_o, z_o)$ and $g(\vec{\kappa}_i, \omega_i; \vec{\rho}_2, z_2)$ are the Green's functions evaluated by propagating the signal from the output plane of the two-photon source to the object plane and the idler from the output plane of the two-photon source to a CCD, where $\vec{\rho}_o$ defines the transverse coordinates of the object

plane.[16,17] Consider that an arbitrary phase of $\Delta\phi(\vec{\rho}_o)$ is introduced on the transverse coordinates of the object plane $\vec{\rho}_o$ by disturbances around the object. Then the two-photon wavefunction becomes:

$$\Psi'(\vec{\rho}_o;\vec{\rho}_2) = \Psi_o \int d\vec{\kappa}_s d\vec{\kappa}_i \delta(\vec{\kappa}_s + \vec{\kappa}_i) \int d\omega_s\, d\omega_i \delta(\omega_s + \omega_i - \omega_p) \times g(\vec{\kappa}_s, \omega_s; \vec{\rho}_o, z_o) e^{i\Delta\phi(\vec{\rho}_o)} g(\vec{\kappa}_i, \omega_i; \vec{\rho}_2, z_2). \quad (6)$$

Since $G^{(2)}(\vec{\rho}_o;\vec{\rho}_2) = |\Psi'(\vec{\rho}_o;\vec{\rho}_2)|^2$, the disturbances have no effect on the formed ghost image in terms of coincidences. After simplification and using the modified Gaussian thin-lens equation shown in Eq. (1) in Eq. (5), we obtain the generalized two-photon effective wavefunction for this case as:

$$\Psi(\vec{\rho}_o;\vec{\rho}_2 = \vec{\rho}_i) \propto somb\left[\frac{R}{c}\left(\frac{\omega_s}{s_o}\vec{\rho}_o + \frac{\vec{\rho}_i}{\frac{d_1}{\omega_s} + \frac{d_2}{\omega_i}}\right)\right], \quad (7)$$

where the point-spread function $somb(x)$ is a result of the finite size of the lens (radius R) and $\vec{\rho}_i$ defines the transverse coordinates of the image plane.

A collection lens along with detector D_1 can be treated as a bucket detector, which is shown in Figs. 1 and 2. The single photon detectors used in quantum imaging are usually very fast, have low dead time, high time resolution, and support high count rates (typically 32 ns dead time, 300 ps timing resolution, and also support up to 30 million counts/s). These features of single-photon detector allow fast accumulation of necessary counts. These features of single-photon detectors allow fast accumulation of necessary counts. Fast single photon detectors allow an integration time of approximately a few minutes for the reported quantum microscopy. Generally, this integration time is less than the life time of the specimen. Faster detection methods currently in development, such as those described by Pittman,[18] will further reduce the integration times needed for quantum microscopy. The bucket detector integrates all $\Psi(\vec{\rho}_o;\vec{\rho}_2 = \vec{\rho}_i)$ reflected and scattered from the object aperture $A(\vec{\rho}_o)$ as a joint-detection event. This process can be written as in the following convolution:

$$R_{12} \propto \int_{\text{object}} d\vec{\rho}_o |A(\vec{\rho}_o)|^2 |\Psi(\vec{\rho}_o;\vec{\rho}_i)|^2, \quad (8)$$

where the CCD is scanned in the image plane $\vec{\rho}_2 = \vec{\rho}_i$. The image is observed in terms of coincidence counts (R_{12}) as a function of the transverse plane coordinates of the CCD ($\vec{\rho}_2 = \vec{\rho}_i$).

The finite size of the image spot defined by a point-spread function in Eq. (7) determines the angular resolution of the imaging. According to Rayleigh's criterion, the images of two nearby point objects are said to be unresolvable when the center of one point-spread function falls on the first minimum of the point-spread function of the other. To clarify this situation, consider a point located at $\vec{\rho}_o = 0$ on the object plane. The corresponding unique spot in the image plane is determined by the point-spread function defined in Eq. (7). Rayleigh's criterion defines the size of the point-spread function by considering its first minimum, i.e.,

$$\frac{R}{c\left(\frac{d_1}{\omega_s} + \frac{d_2}{\omega_i}\right)} \Delta|\vec{\rho}_i| \simeq 3.83 \quad \text{or} \quad \Delta|\vec{\rho}_i| \simeq 3.83 \frac{c}{R}\left(\frac{d_1}{\omega_s} + \frac{d_2}{\omega_i}\right). \quad (9)$$

Now, we consider another nearby point on the object plane at $\vec{\rho}_o = \vec{a}$. In order to separate the image of $\vec{\rho}_o = \vec{a}$ from that of $\vec{\rho}_o = 0$, the value of $m|\vec{a}|_{\min}$ cannot be smaller than $\Delta|\vec{\rho}_i|$, and hence

$$m|\vec{a}|_{\min} \geq 3.83 \frac{c}{R}\left(\frac{d_1}{\omega_s} + \frac{d_2}{\omega_i}\right), \quad (10)$$

where $m = |\vec{\rho}_i|/|\vec{\rho}_o| = [(d_1/\omega_s) + (d_2/\omega_i)]/(s_o/\omega_s)$, is the magnification factor of the image. Thus, we have the angular limit of spatial resolution for two color ghost imaging as

$$\Delta\theta_{\min} = \frac{|\vec{a}|_{\min}}{s_o} = \frac{3.83c}{R}\frac{1}{\omega_s}. \quad (11)$$

Last, under the approximation $d_1 \ll d_2$, the two-photon effective wavefunction becomes

$$\Psi(\vec{\rho}_o;\vec{\rho}_2 = \vec{\rho}_i) \propto somb\left[\frac{R}{c}\left(\frac{\omega_s}{s_o}\vec{\rho}_o + \frac{\omega_i}{s_i}\vec{\rho}_i\right)\right], \quad (12)$$

with the modified image forming equation as

$$\frac{1}{s_o} + \frac{1}{s_i \frac{\omega_s}{\omega_i}} = \frac{1}{f}, \quad (13)$$

where $s_i \simeq d_2$.

Compared to the degenerate ghost imaging system[17] and classical imaging system, we found three interesting features for this quantum microscope system.

1. An angular limit of resolution that is determined by the wavelength of the signal λ_s:

$$\Delta\theta_{\min} = \frac{|\vec{a}|_{\min}}{s_o} = \frac{3.83c}{R\omega_s} \simeq 1.22\frac{\lambda_s}{D}, \quad (14)$$

where D is the diameter of the imaging lens.

2. A different image forming equation: As shown in Eq. (13), the image plane must be moved away from the imaging lens by a factor of ω_i/ω_s in order to form an image when the focal length of the imaging lens f and the object distance $s_o = s_o^O$ are kept the same as in the degenerate case:

$$s_i = \frac{\omega_i}{\omega_s} s_i^O. \quad (15)$$

3. The same imaging magnification factor as that of the degenerate case, with imaging amplification affected by a factor of ω_s/ω_i:

$$\frac{|\vec{\rho}_i|}{|\vec{\rho}_o|} = \frac{\omega_s}{\omega_i}\frac{s_i}{s_o} = \frac{s_i^O}{s_o^O}. \quad (16)$$

Table 1 Comparison of features of microscopes.

Microscope	Resolving power	Contrast	Safety of specimen
Wide-field	R	Noisy	Very high
Confocal	.73R	Very good	Very high
Twin-photon confocal	.17R	Very good	Very low
Noninvasive high resolving power	.4R	Very good	Very high

Comparing the two-color case with the degenerate case and with the classical imaging system with a longer wavelength $\lambda = \lambda_s$, we achieve the same angular resolution limit $\Delta\theta_{\min} = 1.22(\lambda_s/D)$. When the image plane is moved away from the imaging lens by a factor of ω_i/ω_s in order to form an image while keeping the above conditions steady, the imaging amplification increases by a factor of ω_i/ω_s. In this case, the improved amplification factor is 2.5. As stated above, greater imaging amplification under the enhanced resolving power of an imaging system is a useful and important feature in a microscope.

In case of the one-color ghost imaging as well as the classical case, we can resolve $\sim$1 μm with visible light when the object distance (s_o) from the imaging lens is 4 cm. The size of human cells and tissues are of the order of 1 μm. Again, this proposed entangled photon quantum microscope technique would improve the resolving power by a factor of 2.5 over that of a classical wide-field microscope. In this case, the image contrast would be unaffected by disturbances around the object. Furthermore, in this proposed configuration, cells and tissues would be illuminated by visible light instead of UV light, and this would minimize the potential for cell or tissue damage.

4 Comparison of Features of Microscopy

In this section, we present a table to compare the resolving power of different kinds of microscopes in terms of the resolving power of a standard wide-field microscope (R). We also compare the image contrast and specimen safety. The invention of confocal microscopy has provided two important advantages over wide-field microscopes: (1) better resolving power and (2) very good contrast. Later on, the advent of a twin-photon confocal microscope reported improved resolving power significantly beyond the standard confocal microscope. Although twin-photon confocal microscopes can provide very good resolving power, there remains a high probability for cell or tissue damage. In this article, we have reported on a quantum noninvasive, high-resolution microscope that comprises all of the desired features, as shown in Table 1.

5 Conclusion

The main goal of a modern microscope is to achieve high resolving power, high contrast, and noninvasive imaging. Yet, it has been difficult to design a microscope to achieve all of these features together as shown in the comparison of current microscopes above. Nevertheless, the proposed quantum microscope reported here using two-color ghost imaging technology will be able to achieve all the desired features. Here, cells and tissues will be illuminated by one color in the visible range. The resolving power will be determined by the ratio of the signal and idler photon wavelengths, where, for this case, the ratio is 2.5. As a result, the proposed quantum microscope would be noninvasive with high resolving power. In addition, configurations involving virtual images are conceivable, which may increase magnification. Note that in alternate configurations, the resolving power could be improved further by increasing the wavelength ratio of the signal and idler photons since images are formed in terms of coincidence counts between a bucket detector and the CCD. Significantly, image disturbances, such as from motion of intervening fluid in biological samples or from media turbidity, will have virtually no effect on the contrast of the images in this system. We find that such a quantum microscope would be widely applicable in advancing the progress of biomedical research and medical technologies.

Acknowledgments

The authors thank K. Deacon, A. Tunick, P. Hemmer, and J. Sprigg for helpful discussions. S. Karmakar is a postdoctoral fellow at ARL (W911NF-11-2-0074).

References

1. D. S. Simon and A. V. Sergienko, "The correlation confocal microscope," *Opt. Express* **18**, 9765 (2010).
2. D. S. Simon and A. V. Sergienko, "Twin-photon confocal microscopy," *Opt. Express* **18**, 22147 (2010).
3. T. B. Pittman et al., "Optical imaging by means of two-photon quantum entanglement," *Phys. Rev. A* **52**, R3429 (1995).
4. R. E. Meyers, K. S. Deacon, and Y. Shih, "A new two-photon ghost imaging experiment with distortion study," *J. Mod. Opt.* **54**(16), 2381–2392 (2007).
5. R. E. Meyers, K. S. Deacon, and Y. Shih, "Ghost-imaging experiment by measuring reflected photons," *Phys. Rev. A* **77**, 041801 (2008).
6. S. Karmakar and Y. Shih, "Two-color ghost imaging with enhanced angular resolving power," *Phys. Rev. A* **81**, 033845 (2010).
7. S. Karmakar and Y. Shih, "Observation of two-color ghost imaging," *Proc. SPIE* **7702**, 770204 (2010).
8. M. H. Rubin and Y. Shih, "Resolution of ghost imaging for nondegenerate spontaneous parametric down-conversion," *Phys. Rev. A* **78**, 033836 (2008).
9. K. W. C. Chan, M. N. O'Sullivan, and R. W. Boyd, "Two-color ghost imaging," *Phys. Rev. A* **79**, 033808 (2009).
10. R. E. Meyers, K. S. Deacon, and Y. H. Shih, "Turbulence-free ghost imaging," *Appl. Phys. Lett.* **98**, 111115 (2011).
11. R. E. Meyers, K. S. Deacon, and Y. H. Shih, "Positive-negative turbulence-free ghost imaging," *Appl. Phys. Lett.* **100**, 131114 (2012).
12. H. Chen, T. Peng, and Y. Shih, "100% correlation of chaotic thermal light," *Phys. Rev. A* **88**, 023808 (2013).
13. D. N. Klyshko, "Combine EPR and two-slit experiments: interference of advanced waves," *Phys. Lett. A* **132**, 299 (1988).
14. R. J. Glauber, "The quantum theory of optical coherence," *Phys. Rev.* **130**, 2529 (1963);
15. R. J. Glauber, "Coherent and incoherent states of the radiation field," *Phys. Rev.* **131**, 2766 (1963).
16. Y. H. Shih, "Entangled photons," *IEEE J. Sel. Topics Quantum Electron.* **9**, 1455 (2003).
17. Y. Shih, *An Introduction to Quantum Optics*, Taylor & Francis, Boca Raton, Florida (2011).
18. T. Pittman, "It's a good time for time-bin qubits," *Physics* **6**, 110 (2013).

Sanjit Karmakar is a postdoctoral fellow at the U.S. Army Research Laboratory, Adephi, Maryland, USA, and the University of Maryland, Baltimore County, Maryland, USA. He received his PhD in applied physics from the University of Maryland, Baltimore County, USA, in 2012. His current research interests include quantum networks, quantum imaging, and applications of quantum optics in biomedical sciences. He is a member of SPIE.

Ronald E. Meyers is a physicist at the U.S. Army Research Laboratory, Adephi, Maryland, USA. He is a principle investigator in physics research. He has more than 100 scientific publications and more than 20 patents in science and technology addressing significant problems of national interest. His current research interests are focused on fundamental quantum physics, quantum imaging, quantum networking, quantum technology, and quantum information. He is a conference chair of SPIE.

Yanhua Shih is a professor of physics at the University of Maryland, Baltimore County, USA. He received his PhD in physics from the University of Maryland, College Park, USA, in 1987. His recent research interests include fundamental problems of quantum theory, experimental general relativity, quantum information processing, quantum optics, nonlinear optics, and laser physics. He is a conference chair of SPIE.